



저작자표시-비영리-변경금지 2.0 대한민국

이용자는 아래의 조건을 따르는 경우에 한하여 자유롭게

- 이 저작물을 복제, 배포, 전송, 전시, 공연 및 방송할 수 있습니다.

다음과 같은 조건을 따라야 합니다:



저작자표시. 귀하는 원저작자를 표시하여야 합니다.



비영리. 귀하는 이 저작물을 영리 목적으로 이용할 수 없습니다.



변경금지. 귀하는 이 저작물을 개작, 변형 또는 가공할 수 없습니다.

- 귀하는, 이 저작물의 재이용이나 배포의 경우, 이 저작물에 적용된 이용허락조건을 명확하게 나타내어야 합니다.
- 저작권자로부터 별도의 허가를 받으면 이러한 조건들은 적용되지 않습니다.

저작권법에 따른 이용자의 권리는 위의 내용에 의하여 영향을 받지 않습니다.

이것은 [이용허락규약\(Legal Code\)](#)을 이해하기 쉽게 요약한 것입니다.

[Disclaimer](#)

공학석사 학위논문

**Study of 3-Dimensional Magnetic Vortex
State in Magnetic Nano Particles**

자성 나노입자에 형성된 3차원 자기 소용돌이
구조에 대한 연구

2013 년 08 월

서울대학교 대학원
공과대학 재료공학부
이하연

**Study of 3-Dimensional Magnetic Vortex
State in Magnetic Nano Particles**

**A THESIS
SUBMITTED TO THE FACULTY OF SEOUL
NATIONAL UNIVERSITY
BY**

Ha-youn Lee

Supervised by
Prof. Sang-Koog Kim

**IN PARTIAL FULFILLMENT OF THE
REQUIREMENTS FOR THE DEGREE OF MASTER**

August 2013

*Department of Materials Science and Engineering
Graduate School
Seoul National University*

Abstract

Study of 3-Dimensional Magnetic Vortex State in Magnetic Nano Particles

Ha-youn Lee
Department of Materials Science and Engineering
Seoul National University

This thesis deals with statics and dynamics of 3 dimensional magnetic vortices in soft ferromagnetic nanoparticles with micromagnetic simulations and synthesis of permalloy nano particles. For the numerical calculations, the Landau-Lifshitz-Gilbert equation is solved by finite element method (FEM) based micromagnetic simulations using FEMME. Permalloy nanoparticles are prepared by polyol method and analyzed SEM, TEM and XRD to confirm the material properties, such as morphology, crystalline structure of particles.

Nanoparticles are used as the building blocks for different nanostructures such as spherical micelles, vesicles, and cylinders. However, these are notable to bond along specific directions as atoms and molecules.

Self-assembly have been researched intensively within decades even though it is influenced by a number of factors[1].

We observed the arrangements of permalloy magnetic nanoparticle on carbon grid on specific direction by analysis of its models and repetition rate. Magnetic Energy of each arrangement model determine repetition rate

of each arrangement. It is demonstrated with micromagnetic simulation result.

Keywords: magnetic nanoparticles, magnetic vortex, dipolar interaction,

Student number: 2011-20664

Contents

Abstract	1
List of Figures	5
Chapter 1 Introduction	6
Chapter 2 Research Background	9
2.1. Micromagnetics	9
2.1.1. Effective fields in magnetic materials	11
2.1.1.1 Exchange field.....	11
2.1.1.2 Magnetocrystalline anisotropy field.....	11
2.1.1.3 Magnetostatic field.....	14
2.1.1.4 Zeeman field.....	14
2.1.2. Landau-Lifshitz-Gilbert (LLG) equation	15
2.1.3 . Micromagnetic Simulation Method.....	17
2.2.2-Dimensional Magnetic Vortex Structure	21
Chapter 3 Arrangement of Permalloy NanoParticles	26
3.1. Particle Preparation	26
3.1.1. Synthesis of Permalloy nanoparticles.....	26
3.1.2 Properties of nanoparticle.....	29
3.2. Sampling.....	31
3.3. SEM Images of Arrangements.....	33

3.4. Magnetization of Particles with Simulation Results	36
3.4.1. Ground Spin State of Single Magnetic Nano Particle	36
3.4.2. Ground Spin State of Arranged Magnetic Nano Particles ..	39
3.5. Analysis of Pattern Counts and Magnetic Energy	42
Chapter 4 Conclusion	44

List of Figures

2.1	First-order anisotropy energy surfaces for(a)uniform anisotropy (b)cubic anisotropy on $\langle 0 0 1 \rangle$ (c)) cubic anisotropy on $\langle 1 1 1 \rangle$	9
2.2	Schematic illustration of magnetization precession motion around the effective field with damping.....	12
2.3	Schematic illustration of the magnetic vortex structure.....	17
2.4	Schematic illustration of the magnetic vortex core.	8
2.5	Direct measurements of a magnetic vortex structure.....	18
2.6	Energetically equivalent four different states of a magnetic vortex	19
3.1	SEM examination of the Py Nanoparticles.....	22
3.2	Properties of synthesized nano particle.....	24
3.3	Schematic illustration of SEM sample on earth magnet.....	26
3.4	SEM image of some of the arrangements. Arrangement of MNPs.....	29
3.5	Spin configuration at ground state of Py spherical particles	32
3.6	Micromagneticsimulation(FEMME) result	35
3.7	Comparison energy with histogram of assembled pattern models...	37

Chapter 1

Introduction

Fine magnetic particles find extensive application in various fields. Specially, the interest on ferromagnetic metal particles in biology field has been increases, such as nanobiomagnetic applications, including magnetic resonance imaging contrast-enhancement agents, targeted drug delivery, bioseparation and magnetically induced hyperthermia.[2-4] However, since ferromagnetic particles may agglomerate owing to the localized magnetic stray field around particles. Most experimental work so far has used superparamagnetic particles (that is, those with zero magnetic moment at remanence) and their bioconjugates[5]

Magnetic Vortex structure stands out as a solution of this challenge by forming uniform magnetic stray field. The magnetic vortex has been attracted much attention in 2-dimensional disks for its static and dynamic characteristics, *i.e.* for its gyro-motions and reversal behavior under various conditions[6-13] In contrary, the studies on vortex in 3-dimensional object is limited in (quasi-)statics[14-19] and theoretical study in simplified systems[20, 21].

Spin configuration of a magnetic sphere is one of the fundamental questions concerning the single domain size in various materials[22]. In

submicron-sized ferromagnetic elements, the geometrical confinement in nanomagnets alters their energetics from the competition among several magnetic energies: the exchange energy resulting from the wave function of indistinguishable particles being subject to exchange symmetry, the magnetostatic energy due to the classical dipole-dipole interaction between magnetic moments, the magneto-crystalline anisotropy energy from the spin-orbit interaction, and additional energies induced by external forces, such as Zeeman energy. As a result of the competition between these energies, it is known that the spins in a sphere forms a vortex state when the particle size is between the single domain size and multi-domain size [14, 15, 22]. A magnetic vortex is characterized by an in-plane flux-closure spin distribution with net zero magnetization in the absence of a magnetic field and out-of-plane spin distribution [23-27]. This vortex core plays a meaningful role in the arrangement of nanoparticles and dynamic motion of the magnetic vortex structure.

In this paper, we are going to report on the magnetic behavior of soft magnetic spherical particles. Ferromagnetic nanoparticles have strong magnetic energy which governs the arrangement of magnetic nanoparticles. Specially, magnetic vortex spin structure and its vortex core perform as key mechanism of arrangement of magnetic nanoparticles. This statistic study on 3D magnetic vortex would influence to dispersion and arranging method of magnetic nanoparticles.

This thesis is organized as follows. In Chapter 1, the magnetic vortex structure and its static and dynamic properties are introduced. In Chapter 2, we provide the theoretical background to magnetic vortex structure. In Chapter 3 intensive static properties of 3D magnetic vortex with detailed description of 3D magnetic vortex and the interaction between multi- magnetic vortices will be explained. Chapter 4 is about dynamic property of magnetic vortex in magnetic nanoparticle. Finally, chapter 5 is a conclusion of this study.

Chapter 2

Research Background

2.1. Micromagnetics

Micromagnetism is a continuum model of magnetic moments in a ferromagnetic body [28]. In any realistic theory of magnetization processes, all three energy terms: exchange, anisotropy, and magnetostatic, must be taken into account. Until a better theory is developed, the only way to solve the magnetization processes is to neglect quantum mechanics and to use classical physics in a continuous medium. Such a classical theory has been developed in parallel with the quantum-mechanical studies with rough approximation. W.F. Brown gave this theory the name micromagnetics.

Some crystals of specific 3d transition metal such as Fe, Ni and Co have spontaneous magnetic moment even in the absence of magnetic field. These metals easily show ferromagnetic property. Micromagnetics describes the magnetic behavior of ferromagnetic systems by a continuous vector field of classical magnetization vectors [29]. Magnetization vectors are spatial averages of discrete elementary magnetic moments of electron spins. The micromagnetic model is used to describe ferromagnetism semiclassically on length scales of few hundred microns, because of the complexity of calculation on quantum mechanics. Micromagnetism is

considered as it may model not only the static structure of ferromagnets, the formation of magnetic domains and domain walls, but also the dynamics of magnetic structures. The interaction between the magnetization vectors is modeled by effective fields, which is combination of both external applied fields (such as Zeeman field) and internal fields, such as the demagnetization field, exchange field and the magneto-crystalline anisotropy field.

2.1.1. Effective fields in magnetic materials

In the Landau-Lifshitz-Gilbert equation, the effective field H_{eff} is performed as a key element which is a sum of internal effective fields like the exchange H_{ex} , the anisotropy field $H_{\text{anisotropy}}$, and the magnetostatic field H_{d} as well as external fields like the Zeeman field H_{Zeeman} .

2.1.1.1 Exchange field

The exchange energy, a quantum mechanical effect between identical particles, is responsible for ferromagnetism and for the volume of matter. Exchange interaction effects were discovered independently by physicists Werner Heisenberg and P. A. M. Dirac in 1926.[30, 31]

The exchange energy between two magnetization vectors can be derived by starting from the Heisenberg Hamiltonian of two spins S_i and S_j .

$$E_{\text{ex}} = \int_V A_{\text{ex}} \left[(\nabla m_x)^2 + (\nabla m_y)^2 + (\nabla m_z)^2 \right] dV \quad (2.1.1)$$

As exchange constant A_{ex} is expressed as $A_{\text{ex}} = JS^2/a$, and the effective field is the negative variational derivation of the energy, where J_{ij} is the exchange integral, which can be calculated using quantum mechanics.[32, 33]

$$H_{\text{exch}} = - \sum_{i,j=1}^M J_{ij} S_i \cdot S_j \quad (2.1.2)$$

2.1.1.2 Magnetocrystalline anisotropy field

The spin-orbit interaction is the primary source of magnetocrystalline anisotropy field and it can be driven by Maxwell equations.

An instructive way is to expand the free energy in the direction cosines α_1, α_2 and α_3 of the magnetization along the three coordinate axes and apply symmetry operations to reduce the number of independent terms. [34, 35]

$$E_{ani} = K_0 + K_1(\alpha_1^2\alpha_2^2 + \alpha_2^2\alpha_3^2 + \alpha_3^2\alpha_1^2) + K_2(\alpha_1^2\alpha_2^2\alpha_3^2) \quad (2.1.3)$$

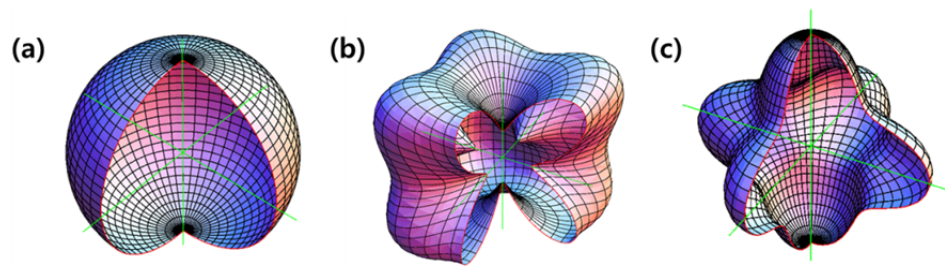


Fig 2.1 First-order anisotropy energy surfaces for (a) uniform anisotropy (b) cubic anisotropy on $\langle 0 0 1 \rangle$ (c) cubic anisotropy on $\langle 1 1 1 \rangle$

2.1.1.3 Magnetostatic field

Starting from Maxwell's equations and assuming that charges are either fixed or move as a steady current. The magnetostatic equations, in both differential and integral forms, are shown as,

$$\nabla \times H_d = 0 \quad \text{and} \quad \nabla \times B_d = 0 \quad (2.1.4)$$

Accordingly, the typical magnetostatic field on magnetic dipole is expressed as,

$$H_d(r) = \int_V \frac{(r-r') \nabla \cdot M(r')}{|r-r'|^3} dV' + \int_S \frac{(r-r') M(r') \cdot n}{|r-r'|^3} dS' \quad (2.1.5)$$

2.1.1.4 Zeeman field

The Zeeman effect, named after the Dutch physicist Pieter Zeeman, is the effect of splitting a spectral line into several components in the presence of a static magnetic field. When magnetic material under external field, either electric and magnetic, the external field affects as Zeeman field.

$$E_{Zeeman} = -\mu_0 \int H_{Zeeman} \cdot M dV \quad (2.1.6)$$

2.1.2. Landau-Lifshitz-Gilbert (LLG) equation

In 1935, Landau & Lifshitz[29] introduced an equation to model the precessional motion of magnetization of uniform ferromagnetic element with an effective magnetic field where γ is the electron gyromagnetic ratio and M_s is the saturation value of the magnetization \mathbf{M} .

$$\frac{d\mathbf{M}}{dt} = -\gamma \mathbf{M} \times \mathbf{H}_{eff} \quad (2.1.7)$$

The magnetic moment is linked to the angular momentum by the gyromagnetic ratio,

$$\gamma = \frac{\mu_0 g |e|}{2m_e} = 2.210173 \times 10^5 \frac{m}{As} \quad (2.1.8)$$

Gilbert proposed a phenomenological damping which encounters the gyration for example due to crystal impurities. In the Gilbert form of the Landau-Lifshitz equation, the damping term leads to a motion of the magnetization, perpendicular to the velocity of the magnetization due to the gyration.[34]

$$\frac{d\mathbf{M}}{dt} = -\gamma \mathbf{M} \times \mathbf{H}_{eff} + \frac{\alpha}{M_s} \mathbf{M} \times \frac{d\mathbf{M}}{dt} \quad (2.1.9)$$

In equation (2.1.9), an ordinary differential equation, the Gilbert phenomenological damping parameter α determines the strength of the damping. At equilibrium both terms vanish to get a vanishing torque, which is the case for a collinear alignment of magnetization and effective field.

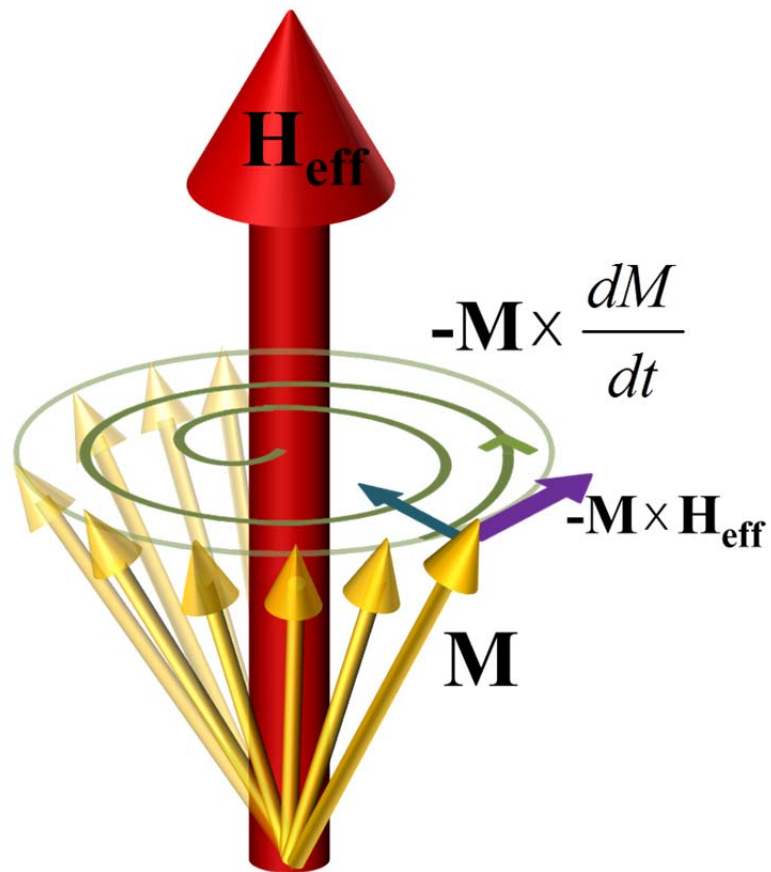


Fig 2.2 Schematic illustration of magnetization precession motion around the effective field with damping.

2.1.3. Micromagnetic Simulation Method

2.1.3.1 Finite element method

The finite element method (FEM) is a numerical technique for solving problems which are described by partial differential equations or can be formulated as functional minimization. A domain of interest is represented as an assembly of finite elements. Approximating functions in finite elements are determined in terms of nodal values of a physical field which is sought. A continuous physical problem is transformed into a discretized finite element problem with unknown nodal values.

For a linear problem a system of linear algebraic equations should be solved. Values inside finite elements can be recovered using nodal values. Two features of the FEM are worth to be mentioned:

1) Piece-wise approximation of physical fields on finite elements provides good precision even with simple approximating functions (increasing the number of elements we can achieve any precision). 2) Locality of approximation leads to sparse equation systems for a discretized problem. This helps to solve problems with very large number of nodal unknowns.

How the finite element method works we list main steps of the finite element solution procedure below.

1. Discretize the continuum. The first step is to divide a solution region into finite elements. The finite element mesh is typically generated by a preprocessor program. The description of mesh consists of several arrays

main of which are nodal coordinates and element connectivities.

2. Select interpolation functions. Interpolation functions are used to interpolate the field variables over the element. Often, polynomials are selected as interpolation functions. The degree of the polynomial depends on the number of nodes assigned to the element.

3. Find the element properties. The matrix equation for the finite element should be established which relates the nodal values of the unknown function to other parameters. For this task different approaches can be used; the most convenient are: the variational approach and the Galerkin method.

4. Assemble the element equations. To find the global equation system for the whole solution region we must assemble all the element equations. In other words we must combine local element equations for all elements used for discretization. Element connectivities are used for the assembly process. Before solution, boundary conditions (which are not accounted in element equations) should be imposed.

5. Solve the global equation system. The finite element global equation system is typically sparse, symmetric and positive definite. Direct and iterative methods can be used for solution. The nodal values of the sought function are produced as a result of the solution.

6. Compute additional results. In many cases we need to calculate additional parameters. For example, in mechanical problems strains and stresses are of interest in addition to displacements, which are obtained after

solution of the global equation system.

2.1.3.2 Micromagnetic Simulation Method

Precise analytical calculation of the magnetization state is possible only for ferromagnetic bodies of high rotational symmetry[36]. For the case of a complex shape, the magnetization state can be solved using numerical computations.

There are three major procedures for numerical computation on magnetic state. First, the ferromagnetic elements are spatially discretized. Second, the effective field is calculated. Third, the main equation- LLG equation is numerically solved.

Magnetic state in spherical magnetic particles, expected by analytic approach is confirmed by finite element method (FEM) based micromagnetic simulations using FEMME[37]. The finite element models made up of surface triangles and volume tetrahedrons let us deal with the precessional motion of the spins in spherical shape properly compared with finite difference method (FDM)[16]. Diameter of the spheres (D) is 80 nm, with the material properties of Permalloy (Py: saturation magnetization $M_S = 860$ emu/cc, crystalline anisotropy $K = 0$, exchange coefficient $A = 13$ pJ/m). The maximum edge length of the tetrahedron was less than 5 nm, which consider the exchange length of Permalloy[38] and is precise sufficient to describe the 3-dimensional vortex cores. Ground spin configurations of the spherical magnetic particles were obtained by relaxing the saturated spheres

to the ground state without external field within considerably enough time (100ns).

2.2. 2-Dimensional Magnetic Vortex Structure

2-dimensional Magnetic vortices are typically observed in patterned or continuous soft magnetic thin films. The magnetic vortex structure consists of in-plane curling and out-of-plane magnetizations at the core region [24, 25, 28, 39]. This out-of-plane magnetization structure is called the ‘vortex core’.

2-dimensional magnetic vortex formation mechanism can be explained by understanding of effective field terms on ferromagnetism. In the absence of any external forces in a soft magnetic nanoelement, Zeeman energy and magnetocrystalline anisotropy energy are negligible. Therefore, the spin configurations are dominantly determined by the competition between the exchange energy and magnetostatic energy. The exchange energy favors electrons with parallel spins. The magnetostatic energy favors closed spin structure to prevent magnetic free poles from generating a stray magnetic field. As a result, magnetizations in the soft magnetic nanoelement are formed with an in-plane curling magnetization along the circular boundary, as shown in Fig. 2.3. The exchange energy will be immeasurable at the disk center because the variation of magnetization will be infinite. To avoid this singularity, a few-nm-scale magnetization structure at the disk center has out-of-plane magnetization as shown in Fig. 2.3. Fig 2.4 shows direct measurement results of various vortex structures in nano-films.

This vortex state can discrete not only two discrete states of up- and down-core orientations and two rotation senses (clockwise or counter-clockwise) of the in-plane magnetizations, but also the vortex state is stable in sufficiently small lateral sizes (> 20 nm) and thicknesses (> 2 nm) of nanoelements[40].

As mentioned above, the magnetic vortex structure is characterized by an in-plane curling magnetization of either counter-clockwise ($c = +1$) or clockwise ($c = -1$) orientation (denoted by chirality c) along with an out-of-plane core magnetization of either upward ($p = +1$) or downward ($p = -1$) orientation (represented by polarization p). Combinations of chirality and polarization of a vortex represent the fourfold degenerate state as shown in Fig. 2.6.

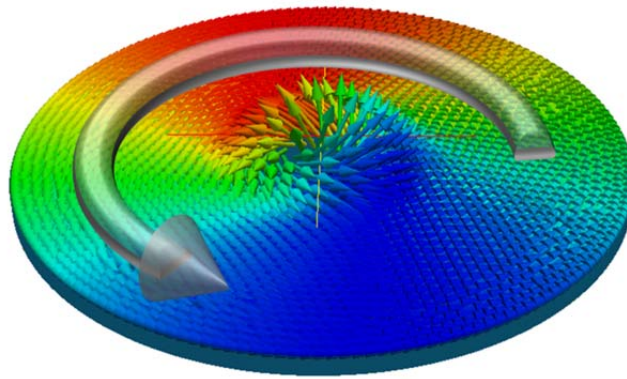


Fig. 2.3. Schematic illustration of the magnetic vortex structure. The magnetizations in a soft magnetic nanoelement are aligned along its circular boundary, forming an in-plane curling magnetization structure around the disk center to prevent magnetic free poles

Out-of-plane M at the core (~10nm)

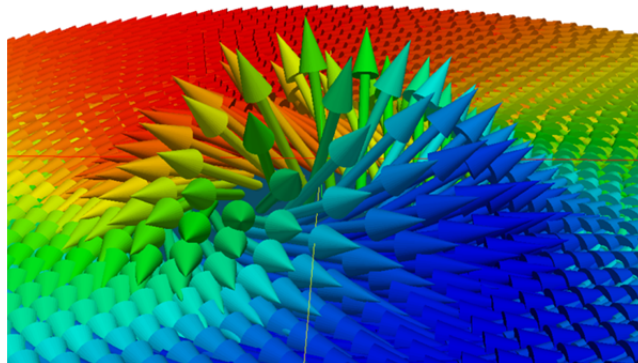


Fig. 2.4. Schematic illustration of the magnetic vortex core. A few-nm-scale out-of-plane magnetization structure at the center of the curling in-plane magnetization structure was developed.

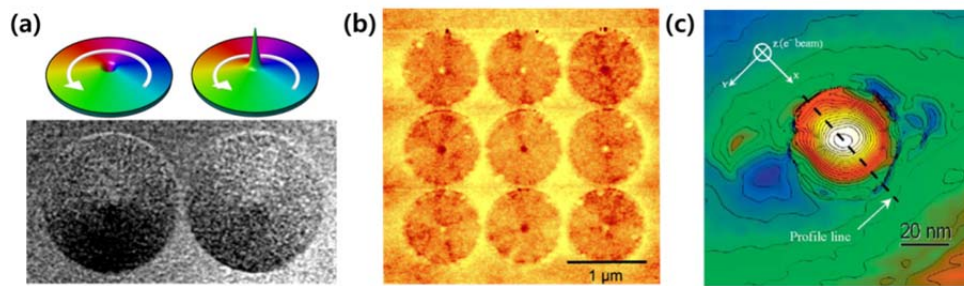


Fig. 2.5 direct measurements of a magnetic vortex structure. (a) Fe L3 edge XMCD images of paired disks, where initial ground states are represented by perspective-view simulation results.[41] (b) Vortex core structure using MFM [24]. (c) Magnetic phase mapping from electron holography: from white to red the magnetisation is rotating from fully out-of-plane (white) to totally in-plane (red).

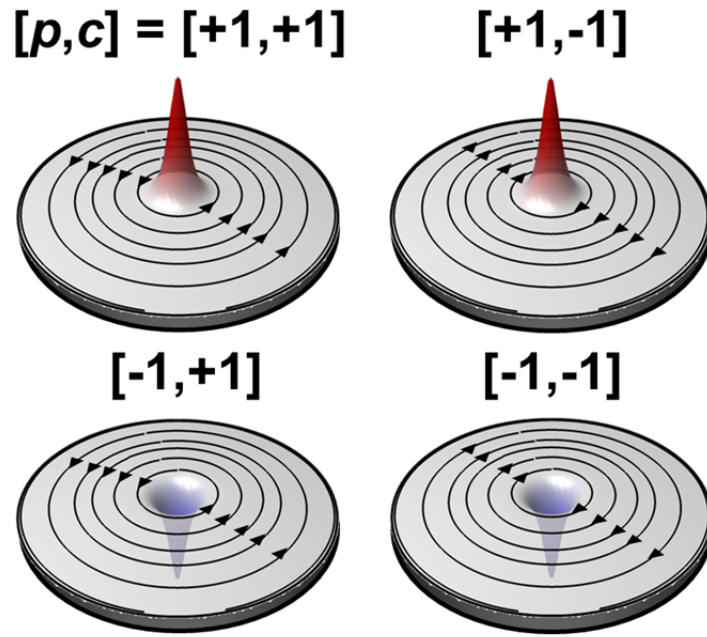


Fig. 2.6 Energetically equivalent four different states of a magnetic vortex according to the vortex core polarization p , and the chirality c . The height and color indicate the local out-of-plane magnetization components.

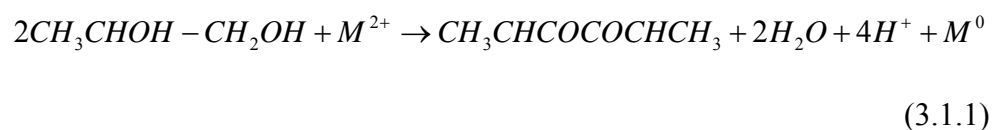
Chapter 3

Arrangement of Permalloy NanoParticles

3.1. Particle Preparation

3.1.1. Synthesis of Permalloy nanoparticles

Spherical Ni₈₀Fe₂₀ permalloy nanoparticles have been prepared by the process known as polyol method. Polyol method is the synthesis of metal-containing compounds in poly(ethylene glycol)s. In this synthesis, the ethylene glycol acts as both the solvent and reducing agent [42]. Even though it is known that the solvents themselves have no reduction ability but they change into propanal during heating. [43-45]



Magnetic nanoparticles have also been frequently synthesized by the reduction of metal salts using reducing agents in the presence of surfactant molecules. [46]

In this polyol process to synthesize Permalloy nanoparticles, Fe, Ni precursors dissolved in propylene glycol at an optimized pH and temperature. Typically 0.1 M FeCl₂, 0.1 M NiCl₂ and NaOH were dissolved in 100 mL propylene glycol (PG) at 80 °C in Ar atmosphere and then heated to 180 °C for 2 h. [47] Same composition of FeCl₂ and NiCl₂ are

participating on this process. Disproportion of iron hydroxide needs to happen since polyols are too weak to reduce Fe ions[44] where Ni reduction occurred easily because of thermodynamic preference. However, disproportionation of ferrous hydroxide happens in reaction, so that Fe particles produced even though iron is too electropositive to be reduced by polyols[48]

Also, it is necessary to note that pH condition acts critically on this synthesis as it is related in metal reduction. As a result of this pH controlling polyol method, the final product has different ratio(1:4=Fe:Ni). Finally, from this synthesis, narrow sized distribution of the final Py nanoparticles with 300nm diameter is obtained (Fig.3.1)

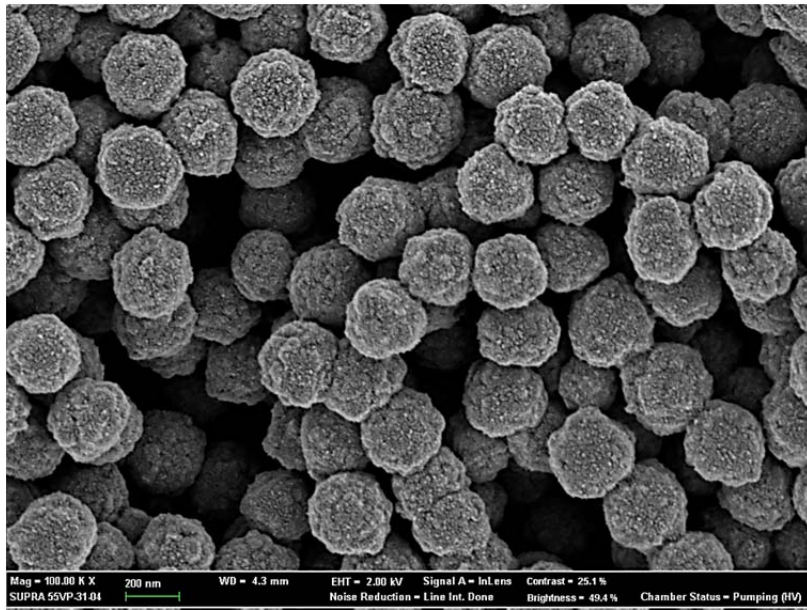


Fig 3.2 SEM examination of the Py Nanoparticles

3.1.2 Properties of nanoparticle

To verify the vortex phenomena in permalloy nanoparticles, SEM/TEM analysis was performed. As previously stated, synthesized particles tend to aggregate in solution. We, therefore, tried to make dispersible particles instantaneously by vortexing machine and sonication. Partially dispersed solution was loaded by drop-casting on Si wafer/carbon grid for SEM, TEM analysis, respectively and dried at room temperature.

Two unique behaviors of the synthesized permalloy nanoparticles were revealed by the HRTEM (High Resolution Transmission Electron Microscope) and SAED (Selective Area Electron Diffraction) analysis. Firstly the particles had poly-crystal features and secondly, the particles had certain assembling patterns during aggregation on the substrate. We believe that these are originated from its own magnetic vortex phenomenon.

Also the crystal structures of Py nanoparticles were determined by X-rayspectrometry(XRD, D8 advance)withCuK radiation at40kV and 40mA. It confirms they have typical FCC structures without any other inclusions

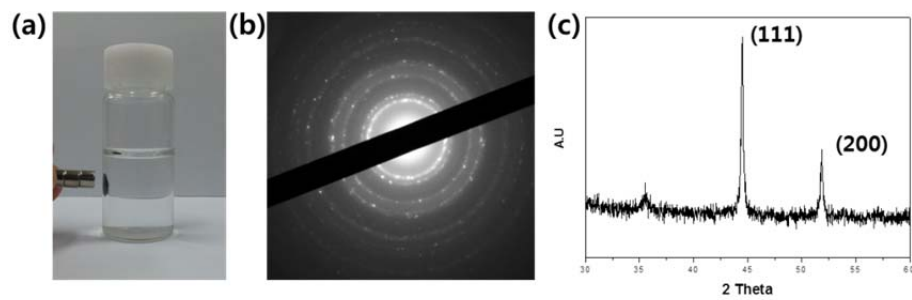


Fig 3.2 Properties of synthesized nanoparticle. (a) Magnetic attraction of nanoparticles by earth magnet. (b) TEM patterns (c) XRD pattern, showing they are of typical FCC structure.

3.2. Sampling

To understand the arrangement mechanism of magnetic nanoparticles, the sampling method needs to be stressed. When magnetic particles interacting each other in the medium without external forces, such as flow of medium occurred by mechanical stirring, Among numerous forced which effect to the arrangements, it is easily imaged that magnetic force acts as key fact of arrangement of ferromagnetic nanoparticles.

In order to observe and research this phenomenon, whole sampling process is performed on the following conditions;

When a drop of medium with magnetic nanoparticle are pose on the substrate, in this research carbon grid, arrangement would occurs immediately and the magnet under the substrate freeze the arranged state of magnetic nanoparticles while avoiding other incidental forces. We then carried out statistical analysis from SEM data to study the ensemble of particles in detail. For the data collection, dispersed permalloy particles were loaded on each ten Si wafers with the same preparation condition. In each samples, 5~60 SEM images were taken randomly. Finally, total 875 images of assembled particles were gathered. The images were classified into small groups with vortex configured criterions.

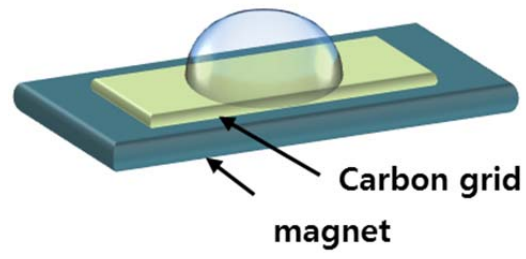


Fig 3.3 Schematic illustration of SEM sample on earth magnet

3.3. SEM Images of Arrangements

Prepared sample is observed by SEM(JSM 5410LV) and specific arrangements are shown on sample. 50~60 samples are analyzed and total 875 arrangements are found and there are, of course, multi-particle aggregation of particles, more than 6 particles are participating, is observed. However, in order to study magnetic vortex state effects on magnetic nanoparticle arrangement, this complex aggregation, more than 6 particles are participating, is not considered.

Representative images of each arrangement are classified with number of particles which are participating on arrangement and its shape(A to G). Not only the observed arrangement but also all the possible arrangements are considered. The possible arrangements of the magnetic nanoparticles which are not observed are schematically illustrated as 5-E to 5-G model.

As shown in Fig 3.4,A-models indicate line-up arrangement. Each arrangements may not form straight line but the diminutive displacement of the particles is ignored and considered as line.

The rest of models are described from 3-B model. For example, 4-B, 4-C,4-E models are the models, which are 3-B model plus a particle and 5-B to 5-D models are the models, which are 3-B model plus 2 particles. On the

other hands, 4-D model is 3-A model plus one and 5-E mole is 3-A model plus 2 particles.

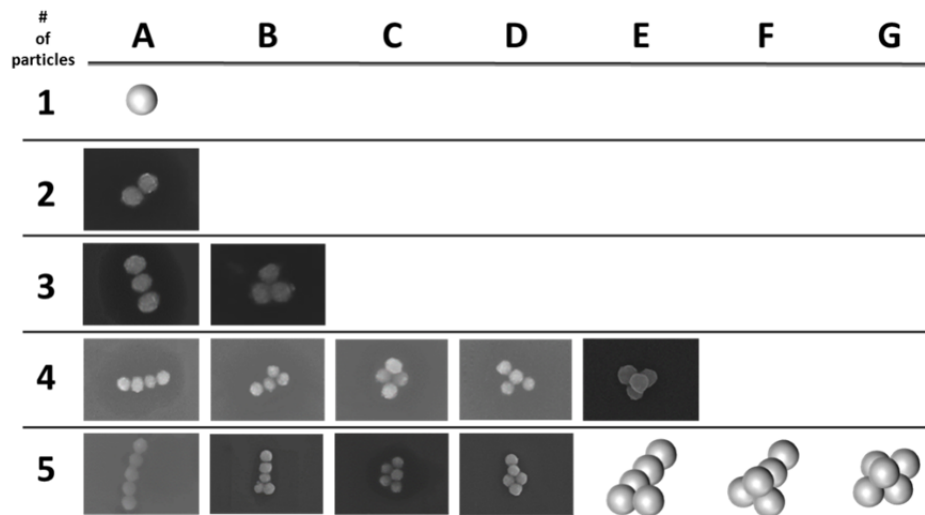


Fig 3.4 SEM image of some of the arrangements. Arrangement of MNPs classified with pattern shape and number of MNPs participating in each pattern. For example, the case of 2-A model, 2 magnetic particles are participating while it clearly forms line shape.

3.4. Magnetization of Particles with Simulation Results

3.4.1. Ground Spin State of Single Magnetic Nano Particle

Magnetic vortex state is formed when reduction of demagnetization energy by circulating spins exceeds gain of exchange energy. According to theoretical calculation(3.1.2), the threshold diameter of Py spheres between the two states(r_c) are known as 25 nm ~ 45 nm, depending on the material parameters, such as A (exchange stiffness), M_s (Saturation magnetization).[14, 16, 22]

$$r_c = \sqrt{\frac{9A}{\mu_0 M_s^2} \left[\ln\left(\frac{2r_c}{a}\right) - 1 \right]} \quad (3.1.2)$$

From our simulations, at $D = 40$ nm the spins at *equator* of the particle starts to lay down on xy -plane from the vortex core direction along the z axis(Fig. 3.5(a), the colors on spheres denotes m_z). The z -component of the equator surface is getting decreased in larger particle, even has negative values when $D \geq 80$ nm. Contrary to the other parts, the spins at the center of the particle are strongly aligned in a direction perpendicular to the rest regions. For $D = 150$ nm the spins inside of the sphere are visualized using streamlines and arrowheads, with the color key for x -component of the spins. The vortex core is shown by iso-surface of $m_z = 0.8$. The interaction between the

magnetostatic energy and exchange energy made the diameter of vortex cores are small at the exposed surfaces (visualized as red dots in Fig. 3.5(a), for $D \geq 50$ nm), and their center thick. The diameter of the vortex core is defined as the full width at half maximum (FWHM) of m_z profile across the equator. Except for the vortex states near the boundary with SD states, the vortex core is proportional to the diameter of particle, as shown in Fig. 3.5(c).

By studying of ground state of Py nanoparticles, particles bigger than $D=80$ nm can be considered as forming same 3-dimensional magnetic vortex state.

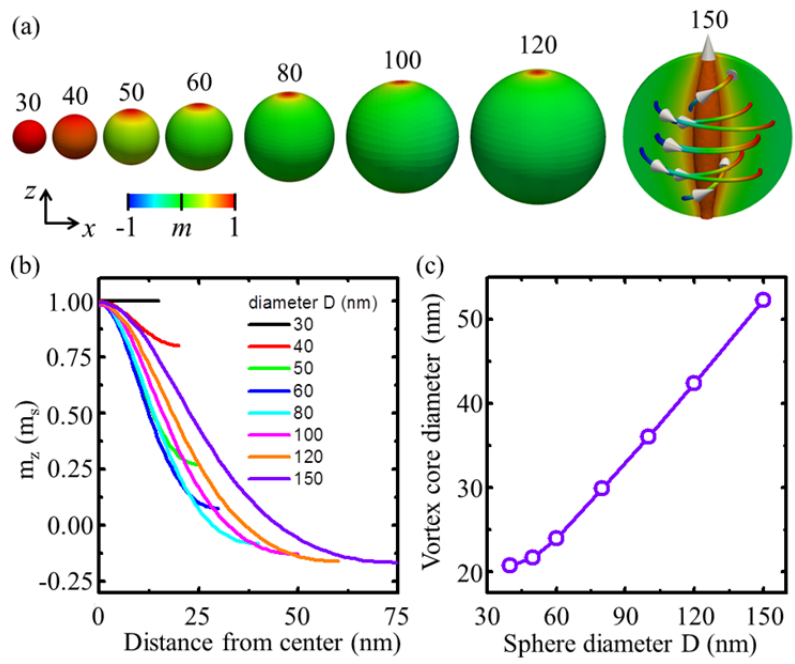


Fig 3.5 Spin configuration at ground state of Py spherical particles for different diameters D (nm) as indicated. The color on the spherical particles indicates m_z as noted by the color bar scale. The arrows inside the sphere $D = 150$ nm represent the direction

3.4.2. Ground Spin State of Arranged Magnetic Nano Particles

All of SEM patterns in Fig 3.4 are simplified as model, for examples, 2-A and 4-B model in Fig 3.6. Micromagnetic simulation performed with this models in conditions that, the particles cannot move after formation of each patterns and the particles in each patterns are having same size, diameter 80nm. Even though synthesized and observed Py magnetic nanoparticles are 300nm, the simulation result with magnetic particles with diameter 80nm can match to the SEM observation with those with diameter 300nm since both of the cases are forming magnetic vortex spin state which acts as key mechanism of formation of particle arrangement.

Number of particles is making the patterns while each of particles maintains magnetic vortex state. Partial spin state changes are shown, on magnetic vortex cores. The magnetic vortex core tends to widen where the magnetic vortex cores are connected. It causes even stronger interaction between the particles.

Among the magnetic energies, those effects on magnetic spin state, demagnetization energy and exchange energy act as more important terms to consider.

A-models, lining arrangement, shows this tendency clearly as all the cores are connected to each other. The direction of magnetic vortex core is parallel to the lined direction to minimize demagnetization energy. On these cases, the magnetic vortex cores can be imagined as bar magnets which has

N,S pole and each N, S pole are connected. However the rotating configuration of spins around vortex core of every particle has same chirality, either CCW or CW, in order to minimize exchange energy of system. When there is particle which is not on the same line than the other particles in the system, as shown in Fig3. 6 (b) particle K, the magnetic vortex core of that particle directs opposite direction to the rest of magnetic vortex core. Also the chirality of rotating spin configuration around vortex core is opposite to the other particles.

While A-models form the line-up configuration of magnetic vortex core and same chirality, models from 4-C is forming rotating configuration of magnetic vortex core and different chirality of rotating spin configuration as shown in Fig3.6 (c). Magnetic vortex cores on 4-C, same as A-models, tend to form tail to tail shape however, since the particles are not linearly located, the magnetic vortex cores cannot line up but rotating.

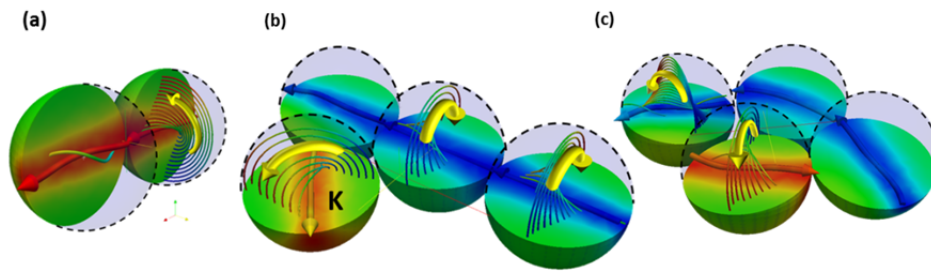


Fig 3.6 (a) Micromagnetic simulation (FEMME) result of 2-A pattern. The color on the half sphere is indicating m_z value, where the red is $+z$ direction and the blue is $-z$ direction. The stream line around magnetic vortex core is colored by m_x value. (b) Micromagnetic simulation (FEMME) result of 4-B pattern. It shows two oriented vortex core and the other core heads opposite direction. (c) Micromagnetic simulation (FEMME) result of 4-C pattern. The magnetic vortex core rotates to make tail-to tail formation.

3.5. Analysis of Pattern Counts and Magnetic Energy

Formation of magnetic vortex state in nanoparticles effects on the arrangement of particles. As the magnetic vortex core tends to appear tail to tail direction to minimize exchange energy of the system, the particles highly prefer to form a line, like shown in Fig 3.6 (a). Meanwhile, 4-C patterns also formed by making tail to tail direction of magnetic vortex core but rotating not lining.

Micromagnetic simulation results not only show spin configuration of magnetic nanoparticles but also the magnetic energy of each patterns

It is necessary to stress that the magnetic energy of ground state of models shows that the model which have smaller magnetic energy have more possibility to be observed. This tendency simply implies that magnetic energy acts as the most effective term on formation of arrangement of magnetic nanoparticles.

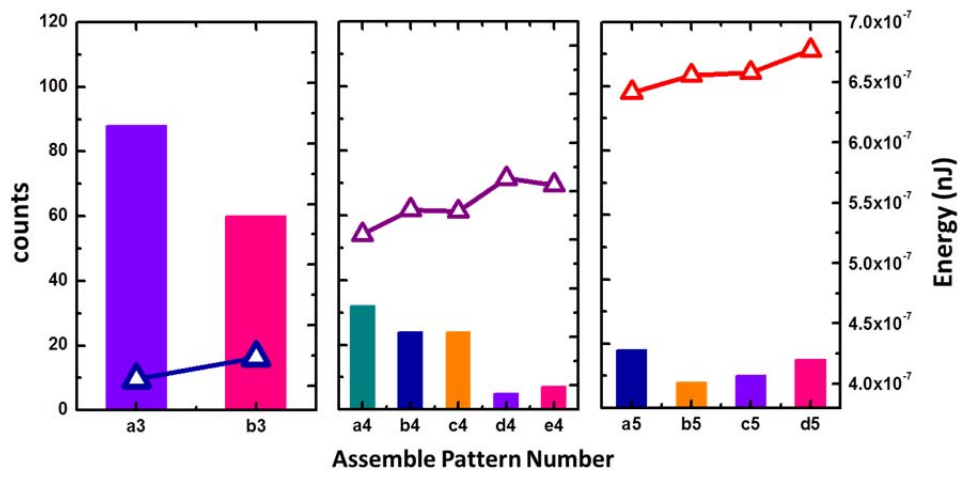


Fig. 3.7 Comparison energy with histogram of assembled pattern models.

Chapter 4

Conclusion

In this thesis, we investigated the 3-dimensional magnetic vortex statics and dynamics in soft magnetic nanoelementsexperimentally and numerically. To understand the underlying mechanism of these interesting properties of the vortex structure, we conducted finite element method (FEM) based micromagnetic simulations using FEMME.

Comparison of SEM image data analysis and magnetic energy of each system proves that dipolar magnetic energy governs the arrangement of magnetic nanoparticles with stable magnetic vortex spin state. This would be demonstrated relation between the magnetic vortex core and arrangement of magnetic nanoparticles.

This thesis not only explains the properties of magnetic vortex states but also as get a foothold of totally different application of ferromagnetic nanoparticles using magnetic vortex, contributes on the future researches on ferromagnetic nanoparticles .

Reference

1. Honggang Cui, Z.C., Sheng Zhong, Karen L Wooley, Darrin J Pochan, *Block copolymer assembly via kinetic control*. Science, 2007. **317**(5838): p. 647.
2. Bruns, O.T., et al., *Real-time magnetic resonance imaging and quantification of lipoprotein metabolism in vivo using nanocrystals*. Nature Nanotechnology, 2009. **4**(3): p. 193-201.
3. Ferrari, M., *Cancer nanotechnology: Opportunities and challenges*. Nature Reviews Cancer, 2005. **5**(3): p. 161-171.
4. Pankhurst, C.E., et al., *Management practices to improve soil health and reduce the effects of detrimental soil biota associated with yield decline of sugarcane in Queensland, Australia*. Soil & Tillage Research, 2003. **72**(2): p. 125-137.
5. Kim, D.H., et al., *Biofunctionalized magnetic-vortex microdiscs for targeted cancer-cell destruction*. Nature Materials, 2010. **9**(2): p. 165-171.
6. Lee, K.-S., et al., *Universal Criterion and Phase Diagram for Switching a Magnetic Vortex Core in Soft Magnetic Nanodots*. Physical Review Letters, 2008. **101**(26): p. 267206.
7. Lee, K.-S., et al., *Ultrafast vortex-core reversal dynamics in*

- ferromagnetic nanodots*. Physical Review B, 2007. **76**(17): p. 174410.
8. Guslienko, K.Y., et al., *Vortex-state oscillations in soft magnetic cylindrical dots*. Physical Review B, 2005. **71**(14): p. 144407.
 9. Guslienko, K.Y., et al., *Eigenfrequencies of vortex state excitations in magnetic submicron-size disks*. Journal of Applied Physics, 2002. **91**(10): p. 8037.
 10. Yu, Y.-S., et al., *Memory-bit selection and recording by rotating fields in vortex-core cross-point architecture*. Applied Physics Letters, 2011. **98**(5): p. 052507-3.
 11. Yu, Y.-S., et al., *Polarization-selective vortex-core switching by tailored orthogonal Gaussian-pulse currents*. Physical Review B, 2011. **83**(17): p. 174429.
 12. Choi, Y.-S., et al., *Out-of-plane current controlled switching of the fourfold degenerate state of a magnetic vortex in soft magnetic nanodots*. Applied Physics Letters, 2010. **96**(7): p. 072507.
 13. Choi, Y.-S., et al., *Understanding eigenfrequency shifts observed in vortex gyrotropic motions in a magnetic nanodot driven by spin-polarized out-of-plane dc current*. Applied Physics Letters, 2008. **93**(18): p. 182508.
 14. Kakay, A. and L.K. Varga, *Monodomain critical radius for soft-magnetic fine particles*. Journal of Applied Physics, 2005. **97**(8): p.

083901-4.

15. Boardman, R.P., et al., *Micromagnetic simulation studies of ferromagnetic part spheres*. Journal of Applied Physics, 2005. **97**(10): p. 10E305-3.
16. Boardman, R.P., *Computer simulation studies of magnetic nanostructures*, in *School of Engineering Sciences*2005, University of Southampton: United Kingdom.
17. Barpanda, P., *Micromagnetics of magnetisation reversal mechanism in Permalloy chain-of-sphere structure with magnetic vortices*. Computational Materials Science, 2009. **45**(2): p. 240-246.
18. Arrott, A.S. and R. Hertel, *Formation and transformation of vortex structures in soft ferromagnetic ellipsoids*. Journal of Applied Physics, 2008. **103**(7): p. 07E739-3.
19. Dimian, M. and I.D. Mayergoyz, *Influence of surface anisotropy on the magnetization precessional switching in nanoparticles*. Journal of Applied Physics, 2005. **97**(10): p. 10J302-3.
20. Shamsutdinov, M.A., L.A. Kalyakin, and A.T. Kharisov, *Controlling the nonlinear dynamics of the magnetization of a small ferromagnetic particle*. Bulletin of the Russian Academy of Sciences: Physics, 2010. **74**(10): p. 1383-1385.
21. Sukhov, A. and J. Berakdar, *Influence of field orientation on the magnetization dynamics of nanoparticles*. Applied Physics A, 2010.

- 98(4)**: p. 837-842.
22. O'Handley, R.C., *Modern Magnetic Materials - Principles and Applications*. 2000: John Wiley & Sons.
 23. Cowburn, R.P., et al., *Single-Domain Circular Nanomagnets*. Physical Review Letters, 1999. **83(5)**: p. 1042-1045.
 24. Shinjo, T., et al., *Magnetic Vortex Core Observation in Circular Dots of Permalloy*. Science, 2000. **289**: p. 930.
 25. Wachowiak, A., et al., *Direct Observation of Internal Spin Structure of Magnetic Vortex Cores*. Science, 2002. **298**: p. 577.
 26. Buchanan, K.S., et al., *Soliton-pair dynamics in patterned ferromagnetic ellipses*. Nature Physics, 2005. **1(3)**: p. 172-176.
 27. Ade, H. and H. Stoll, *Near-edge X-ray absorption fine-structure microscopy of organic and magnetic materials*. Nature Materials, 2009. **8(4)**: p. 281-290.
 28. Hubert, A. and R. Schafer, *Magnetic domains* 1998, Springer, Berlin.
 29. Landau, L.D. and E.M. Lifshitz, *On the theory of the dispersion of magnetic permeability in ferromagnetic bodies*. Phys. Z. Sowjetunion, 1935. **8**: p. 153.
 30. Heisenber, W., *Mehrkr perproblem und Resonanz in der Quantenmechanik*. Zeitschrift f r Physik 1926. **28(6-7)**: p. 411-426.
 31. Dirac, P.A.M., *On the Theory of Quantum Mechanics*. Proceedings of the Royal Society of London. Series A, Containing Papers of a

- Mathematical and Physical Character, 1926. **112**(762): p. 661-677.
32. Spisak, D. and J. Hafner, *Frustrated exchange interactions at the interface of antiferromagnetic films with ferromagnetic substrates: Mn/Fe(100)*. Physical Review B, 1997. **55**(13): p. 8304-8312.
 33. Spisak, D. and J. Hafner, *Theory of bilinear and biquadratic exchange interactions in iron: Bulk and surface*. Journal of Magnetism and Magnetic Materials, 1997. **168**(3): p. 257-268.
 34. Juretschke.h.J., *Crystal physics; macroscopic physics of anisotropic solids* 1974, W. A. Benjamin, Advanced Book Program (Reading, Mass) New York.
 35. Nye.J.F, *Physical Properties of Crystals*. 1957, Oxford, UK: Oxford Univ.Press.
 36. Aharoni, A., *Curling reversal mode in nonellipsoidal ferromagnetic particles*. Journal of Applied Physics, 1999. **86**(2): p. 1041-1046.
 37. Suess, D. and T. Schrefl, *FEMME: Finite Element MicroMagnEtics*, SuessCo: Austria.
 38. Rave, W., K. Ramstock, and A. Hubert, *Corners and nucleation in micromagnetics*. Journal of Magnetism and Magnetic Materials, 1998. **183**(3): p. 329-333.
 39. Kim, S.-K., et al., *Vortex-antivortex assisted magnetization dynamics in a semi-continuous thin-film model system studied by micromagnetic simulations*. Applied Physics Letters, 2005. **86**(5): p.

052504-3.

40. Metlov, K.L. and K.Y. Guslienko, *Stability of magnetic vortex in soft magnetic nano-sized circular cylinder*. Journal of Magnetism and Magnetic Materials, 2002. **242–245, Part 2(0)**: p. 1015-1017.
41. Jung, H., et al., *Tunable negligible-loss energy transfer between dipolar-coupled magnetic disks by stimulated vortex gyration*. Scientific Reports, 2011. **1**.
42. Rahman, P. and M. Green, *The synthesis of rare earth fluoride based nanoparticles*. Nanoscale, 2009. **1(2)**: p. 214-224.
43. Toneguzzo, P., et al., *Monodisperse ferromagnetic particles for microwave applications*. Advanced Materials, 1998. **10(13)**: p. 1032-+.
44. Viau, G., F. Fievet-Vincent, and F. Fievet, *Monodisperse iron-based particles: Precipitation in liquid polyols*. Journal of Materials Chemistry, 1996. **6(6)**: p. 1047-1053.
45. Larcher, D. and R. Patrice, *Preparation of metallic powders and alloys in polyol media: A thermodynamic approach*. Journal of Solid State Chemistry, 2000. **154(2)**: p. 405-411.
46. Frey, N.A., et al., *Magnetic nanoparticles: synthesis, functionalization, and applications in bioimaging and magnetic energy storage*. Chemical Society Reviews, 2009. **38(9)**: p. 2532-2542.

47. Qin, G.W., et al., *Ni₈₀Fe₂₀ permalloy nanoparticles: Wet chemical preparation, size control and their dynamic permeability characteristics when composited with Fe micron particles*. *Journal of Magnetism and Magnetic Materials*, 2009. **321**(24): p. 4057-4062.
48. Viau, G., F. Fievet-Vincent, and F. Fievet, *Nucleation and growth of bimetallic CoNi and FeNi monodisperse particles prepared in polyols*. *Solid State Ionics*, 1996. **84**(3-4): p. 259-270.

초록

자성나노입자에 형성된 3차원 자기소용돌이 구조에 대한 연구

이 논문은 강자성 나노 입자에 형성된 3차원 자기 소용돌이 구조의 거동에 대한 것이다. 최근 나노 구조에 의해서로 다른 결합을 가지는 나노 입자의 특징을 이용하는 자기 조립에 대한 연구가 활발하게 연구되고 있다.

퍼멀로이 나노 파티클의 특징적인 배열과 그 원인으로 밝혀진 3차원 자기 소용돌이 구조에 대한 연구하므로서 자기 조립에 자기에너지가 끼치는 영향을 각 배열의 자기에너지를 전산모사로 계산하고 자성나노파티클을 합성하여 그 배열을 관찰하므로서 증명하였다.

3차원 자기 소용돌이 구조의 거동을 예측하기 위해 LLG 방정식의 해를 유한요소법을 이용하여 도출하는 FEMME 프로그램을 사용하였으며, 폴리올 방법을 이용한 퍼멀로이 나노 입자를 합성하고 SEM, TEM, XRD를 이용하여 합성된 입자의 결정구조와 모양을 증명하였다.

주요어 : 자성나노입자, 자기 소용돌이, 쌍극자 상호작용

학 번 : 2011-20664